21st Australasian Fluid Mechanics Conference
Adelaide, Australia
10-13 December 2018

Experimental study on vortex formation in a screen cylinder wake

T. Zhou[1] and A. Mohd Azmi[2]

[1]School of Engineering, The University of Western Australia,
35 Stirling Highway, Crawley, WA 6009, Australia

[2]Faculty of Mechanical Engineering, Universiti Teknologi MARA, 40450 Shah Alam, Selangor, Malaysia

Abstract

In this paper, wakes generated by a screen cylinder and a solid cylinder have been examined in a wind tunnel over a streamwise range of $5 \leq x/d \leq 60$ (where d is the diameter of the cylinder) at a Reynolds number of 7000 to investigate the vortex characteristics of these bodies. The porosity of the screen cylinder is 58%. The study shows two different regions in the wake of the screen cylinder, namely, the formation region of the large-scale vortical structures and a decaying region of the fully developed large-scale vortices. The former is much longer than that of a solid cylinder wake. The root-mean-square (rms) values of the transverse velocity present a transformation of twin peaks to a single peak which shows the formation of the large-scale vortices from the small-scale vortices in the shear layers. A decreasing trend of the vortex shedding frequency for screen cylinder wake compared to that of a fixed frequency in solid cylinder wake suggests a vortex merging process in the former. The phase-averaging analysis of the spanwise vorticity verifies the presence of the two regions.

Introduction

Vortex shedding is a phenomenon that occurs when fluid flows over a bluff body with certain velocity due to boundary layer separation. It causes a time-dependent variation of pressure on the solid surface, which can introduce many adversative effects on cylindrical structures in a wide range of engineering applications, especially for offshore industry where many cylindrical structures are used. For these structures, if the vortex shedding frequency matches with the natural frequency of the structure, lock-on will occur, resulting in large-amplitude vortex-induced vibrations (VIV).

In order to control vortex shedding and hence VIV, both active and passive methods have been widely used in different situations. Since there are a lot of limitations to the active control, such as high cost and inapplicable for large projects, passive methods seem more preferred, especially for offshore engineering. So far, a large number of researches using passive methods to suppress vortex shedding and VIV for cylindrical structures have been carried out (e.g. Alridge et al. [2]; Kleissl and Georgakis [5]; Zdravkovich [6]; Azmi et al. [3]). Screen shroud is one of the methods proved effective in reducing VIV. Previous studies have shown that a screen shroud of 67% porosity can suppress VIV by about 87% (Acomb [1]).

To explore the mechanism on VIV reduction using screen shroud, in the present study, the wake evolution of a screen cylinder with a porosity of 58% is investigated in a wind tunnel at a Reynolds number Re $(= U_\infty d/\nu)$ of 7000, where d is the diameter of the cylinder, U_∞ is the free stream velocity and ν is the kinematic viscosity of the fluid. It is expected that by examining the formation and evolution of the large-scale vortex structures, some light on the mechanism for VIV reduction using screen shroud can be shed.

Experimental setup

The experiments were conducted in an open circuit wind tunnel with dimensions of 380mm (width) × 250mm (height) × 1840mm (length). The screen cylinder was made up of a woven stainless steel mesh, with a porosity of 58% and wire thickness of 0.36 mm and aperture (a) of 1.25 mm. The mesh was enfolded into a cylindrical structure and tied together with thinnest metal wires with the result of an outer shroud diameter (d) of 20.5mm. Care has been taken to make sure that the diameter of the screen cylinder is uniform along its span. Once the model were rolled and tied, the ends were wrapped against a solid wooden rod before placing into the wind tunnel to prevent any air loss. Wakes of a solid cylinder model was also examined to provide a reference of the expected wake characteristics when compared to the screen cylinder. The solid cylinder was plain and smooth which made up of polished aluminum tube with an outer diameter d of 10.1mm. End plates with dimensions $7d \times 7d$ were used, as shown in Figure 1. Due to the differences of the diameter of the two cylinders, the free stream velocity for the screen cylinder wake is about 5.12 m/s and that for the solid cylinder wake is about 10 m/s, resulting in the same Reynolds numbers for the two tests.

Measurements in the wake were conducted over a streamwise distance of $x/d = 10-60$ with an increment of 5. A hot-wire X-probe was moved across the wake in the y-direction to measure the longitudinal and transverse velocity components, u and v, respectively. Another X-probe was fixed at the wake edge and at the same streamwise location as the first one to provide a phase reference to the measured velocity signals for phase-averaged analysis. The hot wires were etched to a sensor length of 1mm from Wollaston (Pt-10% Rh) wires with a wire diameter of 5 μm, which is long enough to neglect the heat loss at the ends of the sensors. The hot wires were operated with in-house constant temperature circuits at an overheat ratio of 1.5. Angle calibration was performed over $\pm$ 20°. The effective angles of the inclined wires in the two X-probes were 34°, 31°, 37° and 43°. The output signals from the anemometers were low-pass filtered at a cut-off frequency f_c of 5200 Hz. The filtered signals were sampled at a frequency f_s of 10400 Hz into a PC using a 16-bit A/D converter (National Instrument). The sampling period T_s was 30s. Experimental uncertainties were inferred from the estimated inaccuracies in hot-wire calibration data as well as the scatter observed in repeating the experiments a number of times. The uncertainty for the time-average velocity $\overline{U}$ was estimated to be about $\pm 2\%$ while for the fluctuating velocities u and v the uncertainties of their rms values were about $\pm 5\%$ and $\pm 6\%$, respectively. The uncertainty for Reynolds shear stress $< uv >$ was about 8%, where angular brackets denote time averaging. Details of the experiment al setup can be found in Figure 1.

Results and Discussion

In the experiments, the maximum velocity defect was defined as $U_0 = U_\infty - U_{\min}$, where $U_{\min}$ is the minimum velocity across the wake. The wake half width (L) was defined as the distance between the centerline of the wake and the location where the velocity defect was $U_0/2$ (Figure 1). Figure 2 shows the velocity deficits in the two wakes as a function of y^*, where a superscript asterisk denotes normalization by the free stream velocity and cylinder diameter d. It can be seen that the evolution of the velocity

deficits in the two wakes is totally different. For the solid cylinder wake, the velocity deficit decreases slowly with the increase of downstream locations, indicating the recovering process of the wake. The mean velocity deficits in the screen cylinder wake (Figure 2b) reveal a much larger velocity deficit for $x^* < 20$. The velocity gradients in the shear layers over this region are considerably larger than that at other wake locations, associated with the shear layer development. For $x^* \geq 20$, the magnitudes of the velocity deficits are comparable to that in the solid cylinder wake and the velocity profiles become slightly flatter in the central region.

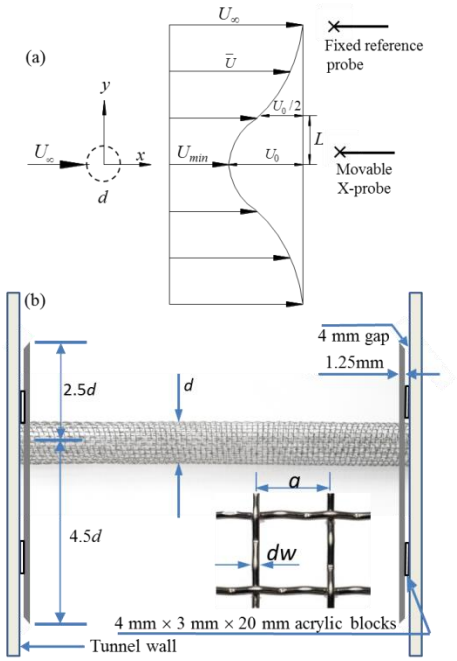

Figure 1. Experimental setup. (a) Wake profile; (b) arrangement of the cylinder.

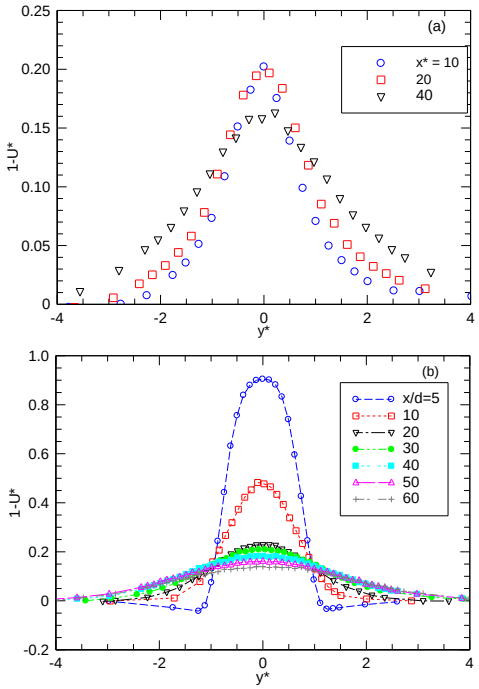

Figure 2. Mean velocity distribution. (a) Solid cylinder wake; (b) Screen cylinder wake.

Results of the root mean square values of the longitudinal (u'/U_∞) and transverse (v'/U_∞) velocities for solid and screen cylinder wakes are shown in Figures 3 and 4, respectively. It can be seem that u'/U_∞ decreases with the increase of streamwise distance in the solid cylinder wake which represents a decay trend of turbulence intensity after the formation, whereas u'/U_∞ in the screen cylinder wake increases as the wake evolves downstream, at least up to x/d = 10. This indicates the enhancement of the turbulence intensity and an expansion of wake region. It shows apparent twin peaks, which occur in the shear layers of the wake. The shear layers for 58% porosity screen cylinder are slightly smaller than that in the screen shroud wake with slightly higher porosity (67%) (Azmi et al. [4]).

For the rms values of the transverse velocity profiles v'/U_∞ (Figure 4), they decrease in the streamwise direction for the solid cylinder wake. On the other hand, the trends revealed by the rms values of the transverse velocity are totally different. They increase in the streamwise direction initially till about x/d = 10, especially in the central part of the wake. The change of velocity profiles from twin peaks to a single peak at x/d = 10 indicates that the large-scale structures may be formed at this location. The magnitude of v'/U_∞ is apparent larger than those in a higher porosity screen cylinder wake (Azmi et al. [4]). After x/d = 10, the magnitude of v'/U_∞ decreases consistently, indicating a decaying process after the formation of the lar-scale vortical structures.

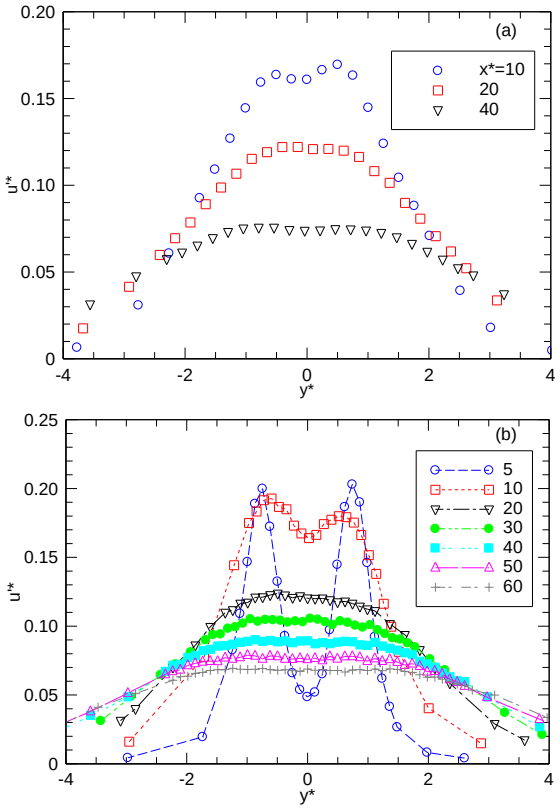

Figure 3. RMS values of the streamwise velocity. (a) Solid cylinder; (b) Screen cylinder.

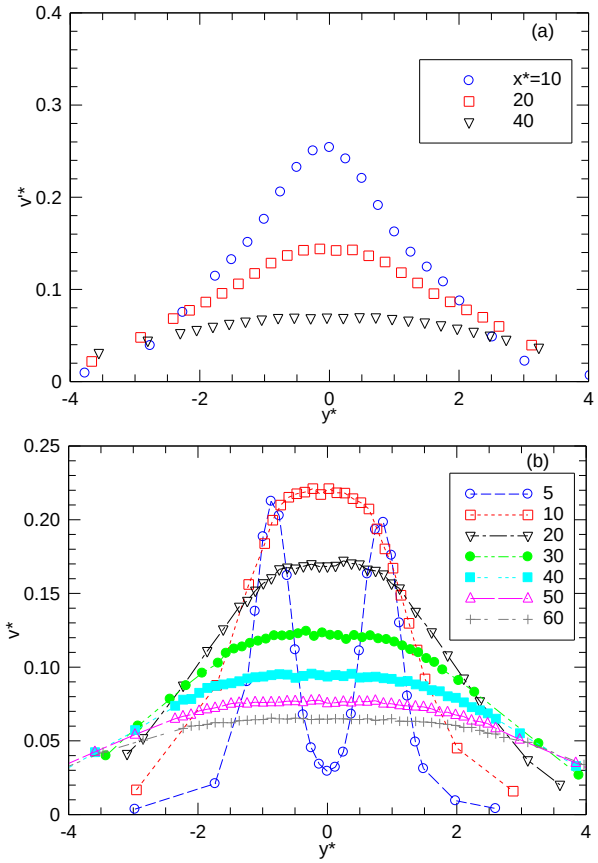

Figure 4. RMS values of the transverse velocity. (a) Solid cylinder; (b) Screen cylinder.

To examining the evolution of the vortex structures in the streamwise direction, energy spectra are shown in Figure 5. They are obtained by conducting FFT to the transverse velocity fluctuations. The frequency is normalized by d and U_∞ so that the peak corresponds to the Strouhal number St. For the convenience to view the spectrum, each spectrum was shifted downward by one order relative to the former location in the figure. For the solid cylinder wake, vortex shedding is apparent, as revealed by a sharp peak at fd/U_∞ = 0.2, corresponding well to the values reported previously. With the increase of downstream locations, the peak height decreases and at about x/d = 40, the peak is nearly indiscernible. Rather, a hump seems to appear with frequency slightly smaller than the vortex shedding frequency, indicating a fast decay of the vortex structures in the solid cylinder wake.

For the screen cylinder wake, however, there is no peak at x/d = 5, but just a broad band hump at fd/U_∞ = 0.3 as indicated by an arrow. At x/d = 10, the hump becomes more apparent and its frequency decreases. The hump becomes more apparent as evolving downstream till x/d = 20. This location is slightly smaller than that for a 67% porosity screen cylinder wake, where the spectrum becomes most apparent at x/d = 30 (Azmi et al. [4]). Similar to the higher porosity screen cylinder wake, the peak frequency here also decreases with downstream locations. This process indicates a long merging process of the small-scale vortical structures in the screen cylinder wake. Due to this merging process, the peak frequency decreases gradually. This is an apparent different process compared with that in a solid cylinder wake. However, it is expected that with the decrease of the screen porosity, the vortex formation region will be shortened.

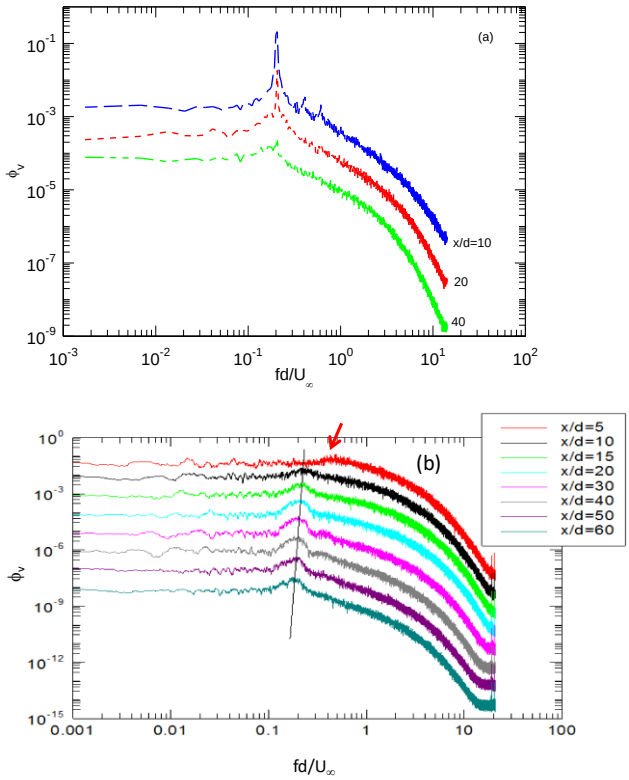

Figure 5. Energy spectra. (a) Solid cylinder; (b) Screen cylinder.

To examine further the vortex formation process, phase-averaged analysis can be used. For a turbulent signal with apparent repeating frequency, the instantaneous signals can be decomposed into three components, namely, a time averaged component $\bar{B}$, a coherent component $\tilde{\beta}$ and the remainder β_r i.e.

$$B = \bar{B} + \beta = \bar{B} + (\tilde{\beta} + \beta_r). \qquad (1)$$

In order to use phase-averaging analysis, the v-signals measured by the reference X-probe was band-pass filtered with the central frequency set at the peak frequency identified on the energy spectra. A fourth-order Butterworth filter was used. The filtered signal was then used to condition the v-signal measured by the movable probe. Details of the phase-average method can be found in Zhou et al. [7]. The iso-contours of the phase averaged spanwise vorticity for solid cylinder wake are depicted in Figure 6 and that for the screen cylinder wake are shown in Figure 7. The phases shown in the figures are ranging from −2 to +2, which correspond to two vortex wave length for convenient viewing of the figure.

The phase-averaged coherent spanwise vorticity in the solid cylinder wake clearly shows the presence of large-scale structures (Figure 6). At x/d = 10, the profile displays the classic Kármán Vortex Street, and the maximum concentration is 0.9. The upper and lower vortices penetrate to the other side across the centerline. It is, therefore, believed that this process is crucial for the decay of the vortices. Actually, the maximum vorticity concentration decreases quickly as evolving downstream, indicating a reduction of vortex strength further downstream. At x/d = 40, the vorticity contours look very irregular.

For the screen cylinder wake at x/d = 5 (Figure 7), the contours of the spanwise vorticity appear only in the upper and lower shear layers, separated by a nearly non-disturbed buffer zone. The small-scale vortices in the shear layers are clearly seen. At x/d = 10, the shear layer vortices become more apparent and increase in size. The range of the shear layers increases. This continues till x/d = 15. At x/d = 20, the buffer layer starts to undulate and the large-scale vortical structures seem to be formed as they are quite

organized at this location, which is consistent with the results indicated by the energy spectra (Figure 5). The interaction between the upper and lower vortices is weak, as reflected by the undulated contours near the wake centerline. As a result, after the formation of the large-scale structures, the vortices decay at a much slower rate as evolving further downstream. In the screen cylinder wake, the maximum concentration decays by 28% from x/d = 30 to 40 while it decays by 56% from x/d = 10 to 20 in the solid cylinder wake, proving that large-scale vortical structures persist longer distance in the screen cylinder wake than that in solid cylinder wake. It is also believed that due to the larger vortex formation length and weaker vortex interaction between the positive and negative vortices, the screen shroud should provide a successful suppression on vortex shedding and VIV.

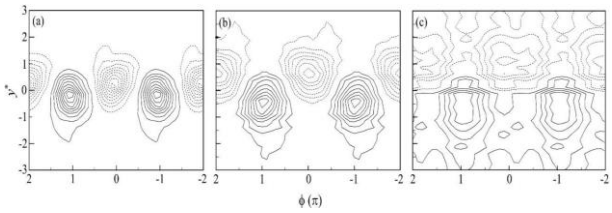

Figure 6. Phase-averaged coherent spanwise vorticity $\tilde{(*)}$ for solid cylinder wake at x/d = 10 (-0.9, 0.9, 0.1), 20 (-0.35, 0.4, 0.05) and 40 (-0.1, 0.1, 0.02).

Conclusions

The wake characteristics of a screen cylinder with porosity of 58% are examined in a wind tunnel at Re = 7000 using hot-wire techniques and the results are compared with that of a solid cylinder wake. The main conclusions are listed below:

- The formation of the vortical structures in a screen cylinder wake has been delayed compared with that in a solid cylinder wake. Small-scale vortices in the shear layers merge together to form large-scale vortices as they evolve downstream.
- When the vortices are large enough, they interact across the centerline, though much weaker than that in the solid cylinder wake, forming the large-scale vortices structures.
- The completion of the formation process may be reflected by the change of the streamwise rms velocities from twin peaks to a single peak at x/d = 20.
- The phase-averaged spanwise vorticity contours verify the existence of two different regions in the wake of screen cylinder, one is the region where small-scale structures are forming into large-scale structures due to merging and the other is the region where large-scale structures have been fully developed. Due to the weak interaction between the vortices across the wake centerline, they decay at a much slower rate compared with that of a solid cylinder wake.

Acknowledgments

The authors sincerely acknowledge the financial support from Australian Research Council through ARC Discovery Projects DP110105171. AMA is grateful to Universiti Teknologi MARA through BESTARI Grant (600-IRMI/DANA 5/3/BESTARI (P) (077/2018)).

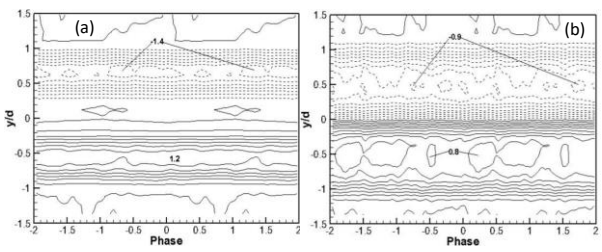

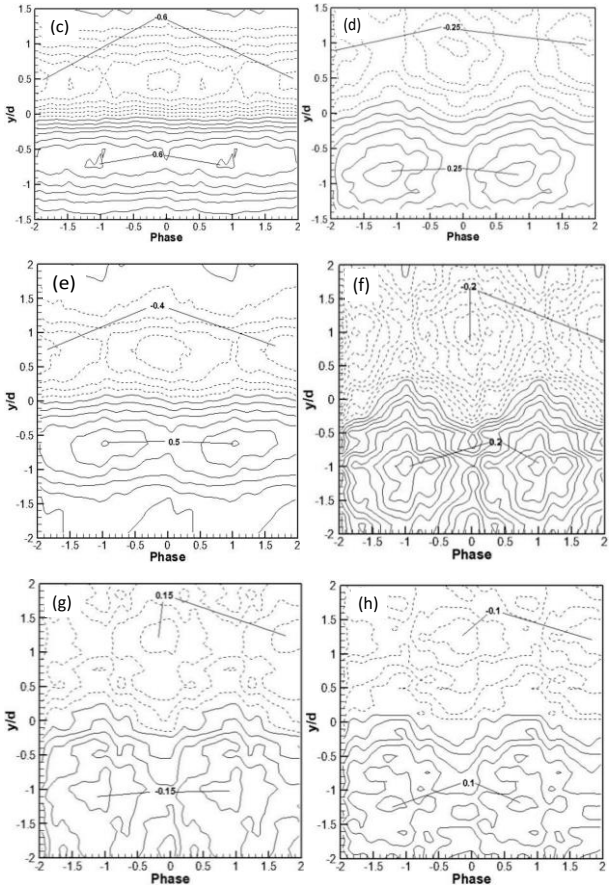

Figure 7. Phase-averaged coherent spanwise vorticity for screen cylinder wake at different downstream locations. (a) x/d = 5; (b) 10; (c) 15; (d) 20; (e) 30; (f) 40; (g) 50 and (h) 60. The numbers inside the figures indicate the maximum contour values.

References

[1] Acomb, S. Suppression of vortex-induced vibration of a cylinder through the use of a meshed shroud with varying porosity, MEng thesis, the University of Western Australia, 2018.

[2] Alridge, T.R., Piper, B.S., Hunt, J.C.R., The drag coefficient of finite-aspect-ratio perforated circular cylinders. J. Wind Eng Ind Aerod. **3**, 1978, 251-57.

[3] Azmi, A.M., Zhou, T., Zhou, Y., Chen, J. and Cheng, L., The effect of a screen shroud on vortex-induced vibration of a circular cylinder and its wake characteristics, In Proceedings of the twenty-fifth International Ocean and Polar Engineering Conference, Kona, Big Island, Hawaii, USA, June 21-26, 2015.

[4] Azmi, A.M., Zhou, T., Zhou, Y., Wang, H. and Cheng, L., Coherent structures in a screen cylinder wake, Physical Review Fluids 3(7), 2018.

[5] Kleissl K. and Georgakis C. T., Aerodynamic control of bridge cables through shape modification: A preliminary study', Journal of Fluids and Structures, 27, 2011, 1006-1020.

[6] Zdravkovich, M.M., Review and classification of various aerodynamic and hydrodynamic means for suppressing vortex shedding, Journal of Wind Engineering and Industrial Aerodynamics, 7, 1981, 145-189.

[7] Zhou, T., Wang, H., Razali, S.F.M., Zhou, Y. and Cheng, L., Three-dimensional vorticity measurements in the wake of a yawed circular cylinder, Physics of Fluids, 22, 2010, 015108.